Applied Clay Science 49 (2010) 348–358

Contents lists available at ScienceDirect

Applied Clay Science

journal homepage: www.elsevier.com/locate/clay

Mineralogical characterization of the fine fraction (<2 μm) of degraded volcanic soils and *tepetates* in Mexico

Claudia Hidalgo [a,*], Jorge D. Etchevers [a], Antonio Martínez-Richa [b], Hernani Yee-Madeira [c], Héctor A. Calderon [c], Ricardo Vera-Graziano [d], Francisco Matus [e]

[a] Colegio de Postgraduados, Campus Montecillo, 56230, Texcoco, Mexico
[b] Facultad de Química, Universidad de Guanajuato, Noria Alta s/n. Guanajuato, Gto. 36050, Mexico
[c] IPN-ESFM, Ed. 9, UPALM, San Pedro Zacatenco 07838 México, D. F., Mexico
[d] Instituto de Investigaciones en Materiales, Universidad Nacional Autónoma de México, Apdo. postal 70-360, Coyoacán 04530, México, D. F., Mexico
[e] Departamento de Ciencias Químicas, Universidad de la Frontera, Av. Francisco Salazar 01145 Temuco, Chile

ARTICLE INFO

Article history:
Received 17 December 2008
Received in revised form 2 October 2009
Accepted 10 November 2009
Available online 26 November 2009

Keywords:
Halloysite
Tepetates
MAS NMR
Mössbauer spectroscopy
HRTEM

ABSTRACT

In Mexico, 70% of the land surface shows some degree of degradation. A substantial portion of these degraded soils are located in the central part of the country, where a high population density exerts unusual pressure on the land. The study of these degraded soils is important because of the ecological, social and economic consequence of this ecosystem component. Two types of degraded volcanic soils were studied in the present research: one coming from *tepetates* (a volcanic tuff, partially altered and ameliorated for production purposes) and the other, a highly eroded Acrisol developed from old volcanic materials. These soils have not been much studied and are here explored due to their potential to sequester carbon. In studies to focus the relationship between mineralogy and the carbon sequestration it will be necessary to clarify the characteristics of the fine fraction of the soil (<2 μm). Clays have been reported to show different mechanisms of association with soil organic matter, in accordance with their nature. In this paper, a mineralogical characterization was made of the fine (2–1 μm) and very fine (< 1 μm) fractions of these soils, considered to be the most active in the sequestration process. The characterization was initially developed by using X-ray diffraction (XRD). However, the results obtained with this technique were not conclusive. In addition, due to the fact that XRD sometimes requires tedious chemical treatments and take time, it is proposed here to use spectroscopical techniques other that the traditional ones to more accurately define the mineralogical characteristics of the studied fractions. The diffuse reflectance infrared Fourier transform (DRIFT), ^{27}Al magic angle spinning nuclear magnetic resonance (^{27}Al MAS NMR), ^{29}Si magic angle spinning nuclear magnetic resonance (^{29}Si MAS NMR), transmission electron microscopic (TEM), high resolution transmission electron microscopy (HRTEM) and Mössbauer spectroscopy were employed.
The fine fractions (<2 μm) of the degraded soils are made up of low activity clays: tubular halloysites in the Te–Tl *tepetates* and kaolinites in the Acrisol. The coarse (2–1 μm) ones in Te–Tl consist also of cristobalite and albite. In Ac–At, akaganeite, goethite and hematite are the principal Fe-mineral components. For this reason, the restoration techniques proposed for these degraded soils must be complemented with appropriate practices of fertilization providing basic elements (Ca, Mg, K and Na) to the soil that can be rapidly lost, and are associated with low activity of the fine fraction.

1. Introduction

Mexico has a surface of 1.97 million square kilometres, of which 64% presents some degree of soil degradation induced by anthropogenic activity (SEMARNAT-CP, 2001). *Land degradation* consists of the permanent or temporary reduction of the productive capacity of land or of its potential for environmental management (FAO, 1979, 1994).

In order to return to degraded soils their role as to the environmental services they should render to ecosystems, whose development took millions of years, it is necessary to have access to techniques allowing to prevent greater degradation, as well as technologies for their recovery. These technologies must start from the knowledge of soil properties and characteristics, particularly from the fraction (≤2 μm) that defined to a greater extent their physical, chemical and mechanic performance.

There are some mineralogical studies of degraded soils in the Mexican High Plateau focused on fraction ≤2 μm (Hessmann, 1992; Hidalgo et al., 1992; Miehlich, 1992; Oleschko et al., 1992; Quantin et al., 1992; Hidalgo, 1996; Hidalgo et al., 1997; Poetsch and Arikas, 1997). Traditional techniques have been used in these studies, like:

* Corresponding author. Tel./fax: +52 595 9511475.
E-mail address: hidalgo@colpos.mx (C. Hidalgo).

0169-1317/$ – see front matter © 2009 Elsevier B.V. All rights reserved.
doi:10.1016/j.clay.2009.11.007

optical microscopy, total chemical analysis techniques and selective dissolution, XRD, microanalysis with EDAX probes and electronic microscopy (MEB, MET and HRTM). Nevertheless, spectroscopy techniques have not been much employed, due to their nature which allow a more detailed depth analysis of the structure of minerals.

The materials selected for this study correspond to two soils derived from volcanic materials with a high level of degradation: an Acrisol, resulting from old volcanic ashes, and a *tepetate*, corresponding to a tuff, fitted out for agricultural activities. Both soils have been studied for their capacity to sequester carbon (Etchevers et al., 2006; Covaleda et al., 2006). The *tepetates* and Acrisol selected for this study are located in the Transvolcanic Mexican Belt (TMB), an area of a high population density that requires cultivation lands for the production of foodstuffs. Thus their agronomic fitting out or recovery becomes necessary to continue contributing to the environmental services of the ecosystems where they are present.

Tepetate is a vernacular Mexican term referring commonly to any type of soil or hardened material. However, a modern scientific definition reserves the term *tepetate* for hardened layers from pyroclastic materials (Etchevers et al., 2006) found in profiles of certain volcanic landscape. The most evident characteristic of the *tepetate* is its hardness. There are two main types of *tepetate:* the duripan and fragipan. The latter is the one that can be broken up to make soil. Similar soil substrates exist in countries around the Pacific fire belt (Zebrowski, 1992, Quantin, 1992). The Acrisols are acid soils that can derive from various types of parent materials, among them, old volcanic ashes.

This study includes the results of the mineralogical analysis of the fine fractions (<2 μm) of these soils under degradation conditions, both with traditional techniques and with techniques not used previously: Mössbauer spectroscopy and nuclear magnetic and ^{29}Si and ^{27}Al nuclear magnetic resonance. The results obtained will allow a more accurate notion of clay materials in these soils, as well as complement the studies over the interactions of these with soil carbon in order to explain the phenomenon of carbon sequestration by the soil.

2. Materials and methods

2.1. Soil characteristics

Soil samples were obtained from 0 to 20 cm depth at two experimental plots: a *tepetate* (Te–Tl) and an Acrisol (Ac–At) located in Tlalpan (Tlaxcala) and Atécuaro (Michoacan), Mexico, respectively. Both sites are located in the TMB around 300 km apart from one another. The *tepetate* was a neutral material (pH in H_2O 6.6), silty–clayey (37% sand, 33% silt, 30% clay), with low content of total nitrogen (0.04% N) and extractable phosphorus (2 ppm, P-Olsen) and a cation exchange capacity (CEC) of 19 cmol kg^{-1}. In the exchange complex Ca (7 cmol kg^{-1}) and Mg (6 cmol kg^{-1}) predominate, bases coming from the weathering of primary minerals. The Acrisol was a soil with acid characteristics (pH in H_2O 5.6), and of clayey texture (65% clay) and high concentrations of total nitrogen (0.16%) and extractable phosphorus (24 ppm P-Olsen) due to the agronomic management given to it and a cation exchange capacity of 19 cmol kg^{-1}.

2.2. Preparation of materials

The soil samples were air dried and then sieved through a sift with 2 mm openings. Organic matter was removed by oxidation with 30% H_2O_2. A pretreatment in cold with H_2O_2 at 30% was initially carried out for one night. Then this reactive was added in portions of approximately 10–20 ml three times a day, shaking them constantly, at about 50 °C, not exceeding 60°, and cooling them down at night. The addition of H_2O_2 was suspended when there was no effervescence after adding one new portion of the reactive and the suspension became clear. Later on the sample was rinsed with distilled water until the reactive was completely eliminated. Clay-aggregate fractions (2–1 μm and <1 μm) for Te–Tl and (<2 μm) for Ac–At were separated from aqueous suspensions by a sedimentation procedure (Stokes' law). The separated clay-aggregate fractions were analyzed for clay minerals and associated impurities. The distribution of the particle-size fraction <2 μm was determined using a Laser Granulometer (Mastersizer, Malvern Instruments). This determination was performed in the LTHE, Grenoble, IRD-France.

Due to the fact that the chemical and mineralogical characteristics of the soils studied (Te–Tl and Ac–At) differ substantially, to study the fine fraction (<2 μm) of both soils, analytical techniques were selected in accordance with the nature of the material. In both cases, X-ray diffraction and infrared spectroscopy (DRIFT) were used. But as these techniques did not allow to accurately identify the fine fraction (<2 μm) complementary techniques were employed, namely, for Te–Tl the transmission electron microscopic (TEM–HRTEM) and, the ^{29}Si and ^{27}Al magic angle spinning neutron magnetic resonance (^{29}Si MAS NMR and ^{27}Al MAS NMR), and for Ac–At, the chemicals analyses and the Mössbauer spectroscopy, so as to identify the nature of the iron compounds present in the soil.

2.3. Chemical analyses

Total soil from Ac–At was treated with chemical extractants to identify the chemical nature of iron compounds in the soil. Acid ammonium oxalate (OX) was used to extract poorly crystallized iron oxides (Van Reeuwijk, 1995). The DCB (dithionite–citrate–bicarbonate) procedure of Mehra and Jackson (1960) was used for the complete dissolution of all crystalline iron oxides and oxyhydroxides. Sodium pyrophosphate (PYR) (Van Reeuwijk, 1995) was used to extract Fe, Al and Si from organic matter materials.

2.4. X-ray diffraction

The clay fractions of Te–Tl (2–1 μm and <1 μm) and Ac–At (<2 μm) were analyzed in the form of powder by XRD on Bruker-AXS, D8 Advance apparatus, with an X-ray copper tube with white incident radiation in the Kα line, at a wavelength of 1.5406 . All analyses were performed at room temperature. The $d(hkl)$-spacings and reflection intensities were measured in Te–Tl diagrams with a scanning speed of 1° (2θ)/min, an angular interval of 2>2θ>70 and the software Diffrac-Plus Release 2000. In the case of Ac–At slides were step-scanned from 5 to 110° 2θ with steps of 0.025° 2θ at 15 s intervals using a voltage of 35 kV, a current of 30 mA and a secondary graphite monochromator.

In addition, in these samples Te–Tl (2–1 μm and <1 μm fractions) and Ac–At (<2 μm fraction) oriented clay specimens were prepared on glass slides: air dried (Or), after ethylene-glycol solvation (EG) and after heating treatments at 350 °C and 490 °C (H). Ultrasonic treatment was used to obtain good particle dispersion. In this case, the irradiation was undertaken using a Shimadzu 5A diffractometer using Cu-K_α radiation at a setting of 40 kV and 20 mA. A divergence slit and angular interval of 2>2θ>35 was used. Minerals and clay fractions were identified from the oriented and random powder diffraction patterns following the procedures given by Brown and Brindley (1980) and Moore and Reynolds (1997).

2.5. Infrared spectroscopy (DRIFT)

A structural characterization of Te–Tl (<1 μm and 2–1 μm) and Ac–At (<2 μm) clay fractions was carried out by Fourier transform infrared spectroscopy using diffuse reflectance (DRIFT). For this, 2.5 mg of pretreated fraction (<2 μm) were mixed with 997.5 mg of KBr. The mixture sample-KBr was heated overnight at 110 °C prior to

analysis, in order to remove the hygroscopic water. The KBr spectrum was subtracted from sample spectra. The spectra were recorded in the range of 4000–370 cm^{-1} on a Thermo Nicolet Nexus Spectrometer, with 64 scans, and a resolution of 4 cm^{-1}.

2.6. Transmission electron microscopic (TEM–HRTEM)

The microscopic and HRTEM observations only from Te–Tl (<1 μm and 1–2 μm fractions) were performed on a JEM 2010 FasTem analytical Microscope working at 200 kV. It is equipped with GIF (Gatan Image Filter) and Z-contrast annular detectors. High resolution TEM (HRTEM) images were obtained at the optimum focus condition.

2.7. ^{29}Si and ^{27}Al-magic angle spinning neutron magnetic resonance (^{29}Si MAS NMR and ^{27}Al MAS NMR)

Solid-state ^{29}Si and ^{27}Al MAS NMR spectra were recorded under proton decoupling on a Varian Unity *Plus* 300 spectrometer only from Te–Tl (<1 μm and 1–2 μm fractions). The unit was operated at 59.58 MHz for ^{29}Si and at 78.18 MHz for ^{27}Al. Approximately 150 mg of the solid sample was packed into a 7-mm-diameter zirconium rotor with Kel-F packs. The rotor spin rate was 5 kHz. For ^{29}Si MAS NMR spectra, a delay time of 6 s was used and 6000 transients were accumulated. For ^{27}Al, a delay time between 0 and 2 s was used and 2000 transients were accumulated. Chemical shifts were referenced for ^{29}Si to the talc peak at −90 ppm and for ^{27}Al to the $Al(NO_3)_3\ 6H_2O$ peak at 0 ppm (both with respect to TMS), as determined on separate samples.

2.8. Mössbauer spectroscopy

The Mössbauer spectra were obtained in powder only from the Ac–At sample (fraction <2 μm), mounted on plastic circular sample holders. Mössbauer measurements were carried out at a room temperature with a ^{57}Fe in Rh source, using a constant acceleration spectrometer (WISSEL) operated in transmission mode. All Mössbauer spectra were fitted using a least-squares minimization algorithm and Lorentzian lineshapes in order to obtain the value of isomer shift (δ), quadrupole splitting (Δ), hyperfine magnetic field (H_f) and relative area (A). The isomer shift values are reported relative to α-Fe at 298 K.

3. Results

3.1. XRD-powder diagrams

3.1.1. Tepetate (Te–Tl) (<1 μm and 1–2 μm)

The XRD patterns of powder preparation of the fractions <1 μm and 2–1 μm from Te–Tl corresponds to the Fig. 1A, B. The difractograms of the two fractions from Te–Tl (<1 μm and 2–1 μm) were very similar. In the finest fraction (<1 μm) (Fig. 1A) the reflections at 0.74 nm, 0.43 nm, 0.35 nm, 0.25 nm, 0.16 and 0.14 nm were associated with the presence of a 1:1 clay, kaolinite or halloysite ($Al_2Si_2O_5(OH)_4$. In the thicker fraction (2–1 μm) (Fig. 1B) additional reflections indicated the presence of other minerals, like cristobalite (SiO_2) (0.40 nm), albite (Na,Ca) $(Si,Al)_4O_8$ (0.32 nm) and quartz (SiO_2) (0.33 nm).

3.1.2. Acrisol–Atécuaro (Ac–AT) (<2 μm)

The powder diffraction diagram of the fraction <2 μm of Ac–At (Fig. 2) showed that this fraction is made up of goethite FeO(OH) (0.42 nm, 0.27 nm and 0.25 nm), hematite (Fe_2O_3) (0.27 nm, 0.25 nm, 0.18 nm, 0.16 nm and 0.15 nm), akaganeite (FeO(OH) (0.74 nm, 0.33 nm, 0.25 nm, 0.23 nm and 0.16 nm), kaolinite (0.74 nm) and also of quartz (0.42 nm and 0.33 nm) and cristobalite (0.40 nm).

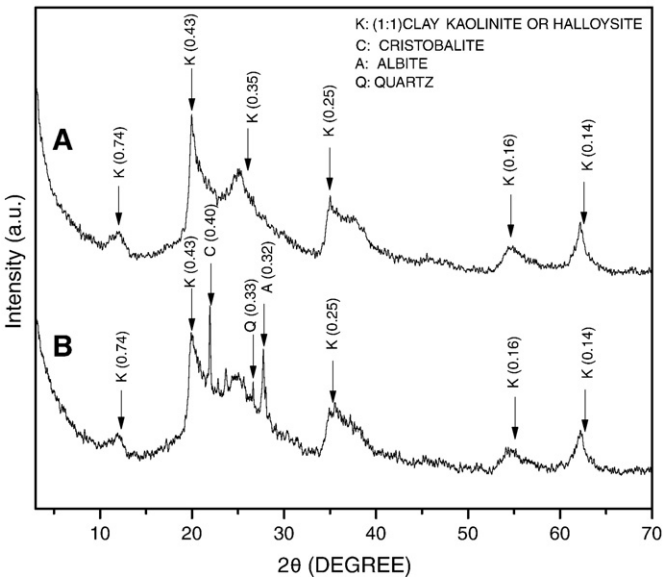

Fig. 1. XRD patterns of powder preparations from Te–Tl, (A) <1 μm and (B) 2–1 μm (Cu-Kα radiation).

3.2. XRD-diagrams in oriented aggregates

3.2.1. Tepetate (Te–Tl) (<1 μm and 2–1 μm)

The diffraction patterns of the oriented aggregate diagrams of both size fractions of the Te–Tl sample (Figs. 3 and 4) proved to be ambiguous, since they can be associated with that of a halloysite-7 Å or a distorted kaolinite (Brindley, 1980; Chen, 1984; Chen et al, 1997). These diagrams are very similar to those presented by Chen et al. (2004) for a 0.7 nm halloysite with a main reflection at 0.735 nm and a broad band at 0.356 nm.

The basal reflection at 0.735 nm is too broad (Figs. 3 and 4) which can be explained by the presence of small-sized crystals (Trunz, 1979), a high degree of disorder, tubular morphology or an interstratification of layers with different degrees of hydration (Brindley, 1980). This reflection is similar to the spacing between 1 and 0.7 nm exhibited by the partially dehydrated halloysite (Moore and Reynolds, 1997) and it corresponds to a partial removal of the interlaminar water layers. In this case the identification may turn out to be more complicated because a peak of 0.745 nm has also been interpreted as an indicator of the

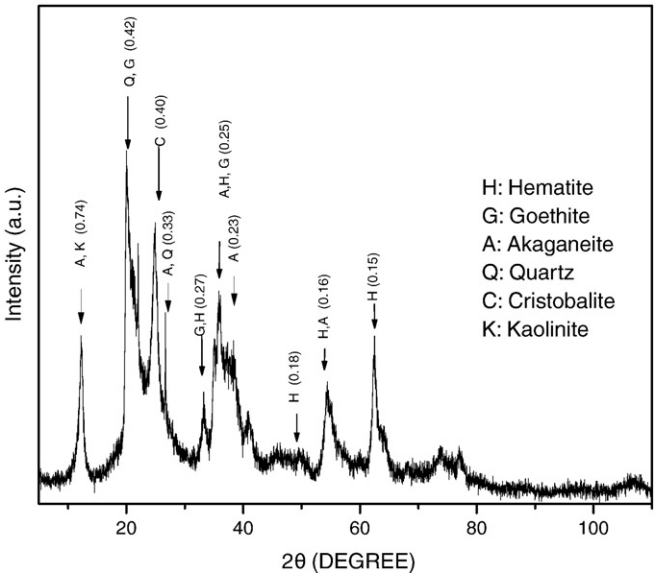

Fig. 2. XRD patterns of powder preparation from Ac–At, <2 μm (Cu–Kα radiation).

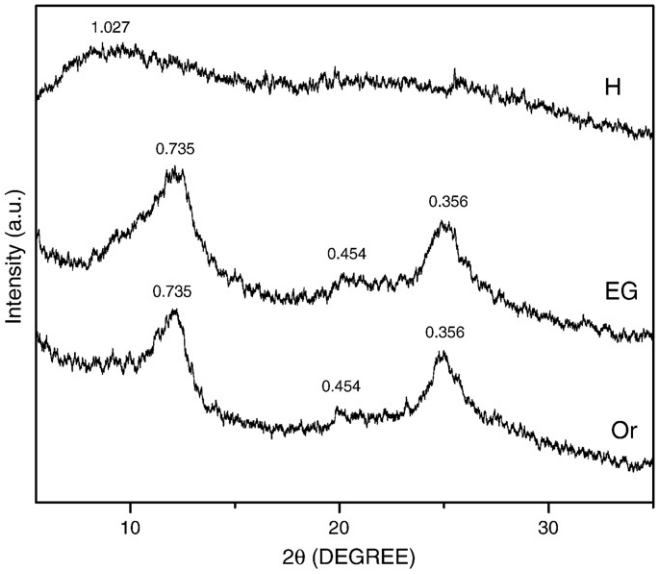

Fig. 3. Oriented diffraction patterns on glass slides of fraction <1 μm (Te–Tl). Or: air dried, EG: after ethylene-glycol solvation, H: heating treatment at 490 °C, (Cu-Kα radiation).

presence of 1:1 random interstratification of kaolinite–smectite (Sawhney, 1989).

A diffuse band between 0.412 and 0.454 nm (*d*) indicates the existence of a high-defect kaolinite. This diffuse band is made up of four XRD peaks and of low resolution reflections, including 020, 110, 111 and 111 (or 02, 11 of the halloysite) (Chen et al., 2004), among others.

Both fractions from Te–Tl (<1 μm and 2–1 μm) maintain the same *d*-spacings after ethylene-glycol treatment (EG) (Figs. 3EG and 4EG), *i.e.* the peaks around 0.735 nm, 0.45 nm and 0.356 nm did not show a shift. A similar performance has been reported for the dehydrated halloysite (Moore and Reynolds, 1997) where a basal spacing close to 0.72 nm is stabilized. This partially dehydrated halloysite did not expand with ethylene-glycol treatment.

The heating at 300–350 °C (not presented) did not lead to the sharpness of the reflections, nor to the reduction of the interlaminar space to 0.714 nm, characteristic value of kaolinite (Brindley and Robinson, 1946), therefore it is possible to come to the conclusion that it is not a kaolinite in both fractions from Te–Tl. In both fractions (<1 μm and 2–1 μm) (Fig. 3H) no peak was detected after a 490 °C heating which confirmed that it is not interstratification of mixed layers (Sawhney, 1989) in these samples. Others peaks were observed in the thicker fraction (2–1 μm) (Fig. 4) corresponding to albite (0.321 nm) and cristobalite (0.404 nm) (see Fig. 1B). The weak signal at 1.016 nm was related to mica structure produced after the heating at 490 °C. The literature on the subject corroborates the above information, and indicates that it is not easy to distinguish between kaolinite and halloysite from the X-ray diffraction patterns (Chen et al., 2004).

3.2.2. Acrisol–Atécuaro (Ac–At) (<2 μm)

The X-ray diffractogram (Fig. 5) showed sharper XRD peaks than the two clay fractions (<1 μm and 2–1 μm) from Te–Tl. The natural preparations in oriented aggregates showed the reflections at 0.736 nm, 0.45 nm and 0.362 nm that did not show a shift as a result of saturation with ethylene-glycol which confirmed the presence of 1:1 clays in this soil (Fig. 5). In this case identification may turn out to be more complicated since a peak of 0.736 nm has also been interpreted as an indicator of the presence of chlorite Fe-rich where 001 and other higher odd-order reflections have weak intensities. Considering that Fe-rich chlorites do not display the 1.4 nm (001) spacing (Barnhisel and Bertsch, 1989), a confusion might occur when differentiating chlorites from kaolinites in this condition. The soil red color is evidence of the presence of Fe-compounds or maybe of Fe-rich clays. The literature reports that the identification of chlorite in a mixture with kaolinite is difficult, especially in soil samples and recent sediments (Barnhisel and Bertsch, 1989). However, the reflections disappeared after heating at 490 °C, corresponding to the disintegration of kaolinite (Holtzapffel, 1985), and Acrisols are characterized to present low activity clays (WRB, I.W.G., 2006), *i.e.* kaolinites (Brady and Weil, 2002).

The results obtained showed that *tepetate* (Te–Tl) (<1 μm fraction) are made up of 1:1 clay minerals similar to halloysite ($Al_2Si_2O_5(OH)_4$ partially dehydrated. The literature on the subject corroborates the above information, and indicates that it is not easy to distinguish between kaolinite and halloysite from the X-ray diffraction patterns (Chen et al., 2004). *Tepetate* (Te–Tl) (2–1 μm fraction) are made up of

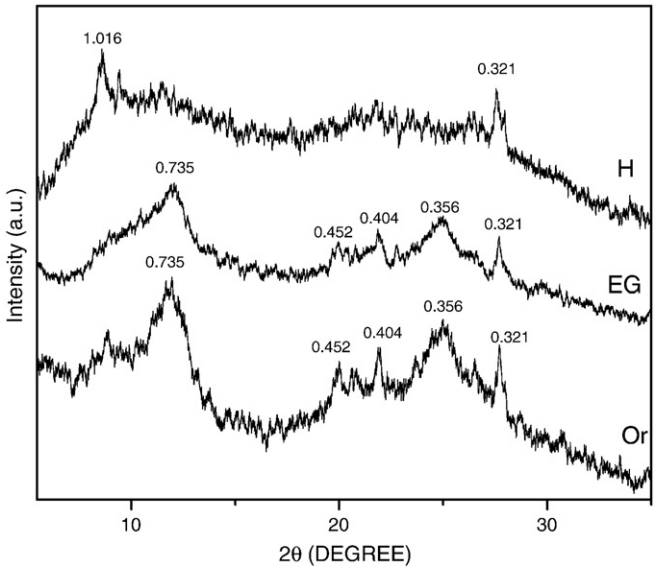

Fig. 4. Oriented diffraction patterns on glass slides of fraction 2–1 μm (Te–Tl). Or: air dried, EG: after ethylene-glycol solvation, H: heating treatment at 490 °C, (Cu-Kα radiation).

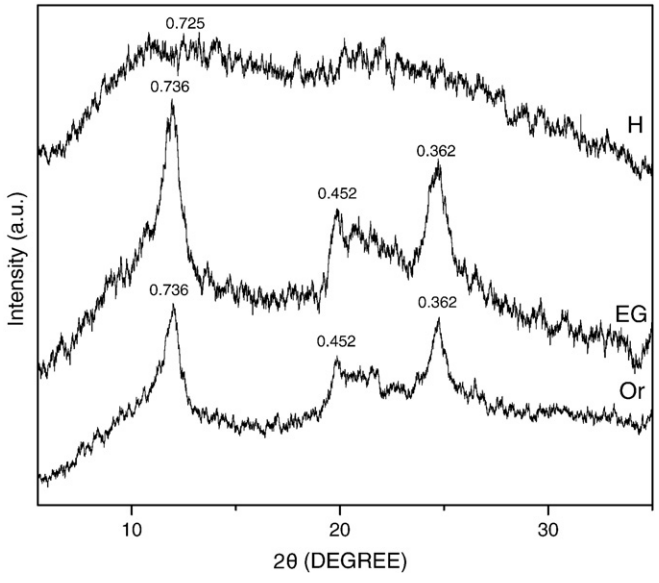

Fig. 5. Oriented diffraction patterns on glass slides of fraction <2 μm (Ac–At). Or: air dried, EG: after ethylene-glycol solvation, H: heating treatment at 490 °C, (Cu-Kα radiation).

1:1 clay minerals similar to halloysite ($Al_2Si_2O_5(OH)_4$. In this fraction there are other minerals present, like cristobalite (SiO_2), albite (Na,Ca) $(Si,Al)_4O_8$ and quartz (SiO_2). Acrisol–Atécuaro (Ac–AT) (<2 μm) is made up of kaolinite and iron oxides and/or oxyhydroxides such as goethite FeO(OH), hematite (Fe_2O_3), akaganeite (FeO(OH) and also of quartz and cristobalite.

3.3. Infrared spectroscopy (DRIFT)

Since the XRD did not allow identification with accuracy the present clays, the study was complemented with IR spectroscopy studies.

3.3.1. Tepetate Te–Tl

The FTIR spectra of the two separated clay fractions (<1 μm and 2–1 μm) are shown in Fig. 6.

In both cases (Fig. 6A and B), it was possible to observe the bands at 3696, 3622, 1035, 912, 752, 688, 540, 471 and 436 cm^{-1}, corresponding to a spectra characteristic of a halloysite (Van der Marel and Beutelspacher, 1976). The bands corresponding to the vibrations Al_2OH-stretching at 3695 cm^{-1} and 3620 cm^{-1} (OH united to Al atoms) (Farmer, 1974; Frost, 1998), presented displaced at 3700 and 3626 cm^{-1}, respectively. The band around the 3700 cm^{-1}, OH-stretching (Farmer, 1979) of the free hydroxyls (Chukhrov and Zvyagin, 1966) or surface OH (Madejová and Komadel, 2005) was reduced by the intercalation of interfoliar water (Quantin et al., 1984; Quantin, 1993). The band at 3626 cm^{-1} was assigned to the stretching vibrations of the internal OH groups of the 1:1 dioctahedral silicated layers linked to octahedral cations (Al^{3+}) (Farmer, 1974) which are associated with hydrogen (Chukhrov and Zvyagin, 1966). Both bands 3700 and of 3626 cm^{-1}, have been reported as characteristic of halloysite (Chukhrov and Zvyagin, 1966; Ross et al., 1983; Joussein et al., 2005). The second band (3626 cm^{-1}) is characteristic of natural spherical halloysites (Wada et al., 1988). The absence of a band at 3657 cm^{-1}, characteristic of the kaolinite, confirmed that the 1:1 clay detected by XRD in <1 μm and 2–1 μm fractions from Te–Tl corresponded to a halloysite. The shoulder about 3426 cm^{-1}, equal to that showing a halloysite of Indiana (Ross et al., 1983), was attributed to the adsorbed residual interlaminar water (Theng et al., 1982; Ross et al., 1983). Within this region, the band at 3550 cm−1, characteristic of the halloysite (0.7 nm), according to Kodama and Oinuma (1963), was not identified in the clays studied.

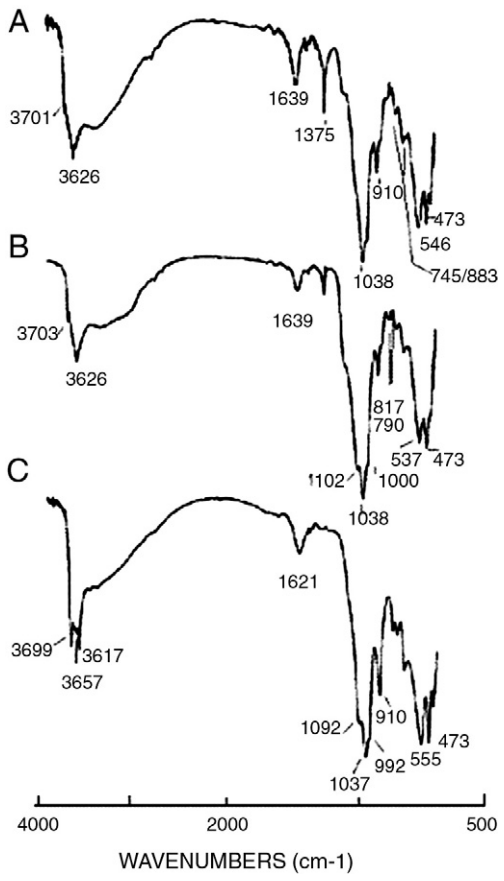

Fig. 6. Diffuse reflectance infrared Fourier transform spectra (DRIFT) of clay fractions. A: <1 μm (Te–Tl), B: 2–1 μm (Te–Tl) and C: <2 μm (Ac–At), (transmittance mode).

The band at 1639 cm^{-1}, attributed to the OH groups of free water, was longer in Te–Tl (2–1 μm) than in Te–Tl (<1 μm), which clearly indicated that in fraction 2–1 μm there is interlaminar water, which leads to a lower degree of ordering of the clay sheets (Bobos et al., 2001). These correspond to the OH-bending frequencies of water.

According to Farmer (1979), the bands between 1000 and 1120 cm^{-1} correspond to the Si–O stretching vibrations. In this region, the two fractions of Te–Tl (2–1 μm and <1 μm) clay showed bands at 1038 and 1000 cm^{-1}. The band at 1038 cm^{-1} was attributed to Si(Al)–O vibrations (Wada et al., 1988) or Si–O vibrations (Chukhrov and Zvyagin, 1966). The sharpness of this band (1038 cm^{-1}) was similar to that of the halloysite reported by Joussein et al. (2005). The greatest difference between the FTIR spectra of the separated clay fractions of the Te–T1 sample was registered in this region; the thicker fraction (2–1 μm) presented a stretching vibration (Si–O) at 1110 cm^{-1}, more evident in this fraction due to the contribution of the present feldspar. This band, jointly with the bending Si–O vibrations at 473 cm^{-1} and Si–O–Si at 790 cm^{-1} are characteristic of the opale-Ct (Fröhlich, 1993). The band at 817 cm−1 corresponds to the bending Si–O–Si vibration of the silica tetrahedron (Fröhlich, 1993). Within the same region, the band at 910 cm^{-1} corresponds to OH-bending vibrations of the internal OH groups (Farmer, 1979; Bobos et al., 2001) united at Al, Al–OH, in the type 1:1 dioctahedral laminar silicates (Chukhrov and Zvyagin, 1966, Farmer, 1974) or Al_2OH-bending (Joussein et al., 2005). This band was identified by Chukhrov and Zvyagin (1966) in halloysites with a high degree of structural disorder in which the doublet at 940–810 cm^{-1}, characteristic of samples of higher crystallinity, was reduced to only one peak between 940 and 910 cm^{-1}, as is the case we are dealing with in this study.

The bands at 683, 546, 473 cm^{-1} observed in the spectrum of Te–Tl (2–1 μm) have also been reported for natural and synthetic spherical halloysites (Wada et al., 1988). However, the features presented in this region are common both for kaolines and spherical halloysites, reason why these bands only allow verifying a structure of present 1:1 layer (Wada et al., 1988). The vibrations around 540 and 470 cm^{-1} were assigned to the Al–O–Si and Si–O–Si bending unions (Farmer, 1979). These have been defined as belonging to well ordered kaolinites (Bobos et al., 2001).

In general, it may be concluded from the FTIR spectroscopy studies that the present clay in the separated fractions of Te–Tl (<1 μm and 2–1 μm) corresponds to a halloysite. The spectrum of both fractions is very similar to that of a halloysite with structural disorder (Chukhrov and Zvyagin, 1966). In the thicker fraction (2–1 μm) (Fig. 6B), it was possible to verify the presence of opal-Ct detected in the X-ray diffraction.

3.3.2. Acrisol–Atécuaro (Ac–At)

In the FTIR spectrum obtained for the fraction <2 μm of Ac–At (Fig. 6C), it was possible to observe the bands associated with the OH-stretching vibrations of the OH–A1 external groups (3699 cm^{-1}) and internal (3617 cm^{-1}), in addition to a small sign of about 3650 cm^{-1}. The profile of these bands was characteristic of that of a disordered kaolinite (Farmer, 1979; Wilson, 1987) in which the band length at 3699 cm^{-1} was detected to be slightly higher to that of 3617 cm^{-1}. At low wave numbers, the bands 1092, 1037, 992, 910, 691, 554, 472 and 427 cm^{-1} were associated with the vibrations –Si–O of the

tetrahedral layer. In general these bands indicate also the presence of a disordered kaolinite (Farmer, 1979, Wilson, 1987). The very long band at 910 cm^{-1} indicated the presence of type 1:1 dioctahedral laminar silicates (Farmer, 1974) or Al_2OH-bending (Joussein et al., 2005). The doublet at 800 and 737 cm^{-1} points to the presence of quartz and opal-Ct. The vibrations about 540 and 470 cm^{-1} were assigned to the Al–O–Si and Si–O–Si bending vibrations (Farmer, 1979). These are defined as characteristic of those of well ordered kaolinites (Bobos et al., 2001). In general, it may be concluded from the FTIR spectroscopy studies that the present clay in the separated fractions of Ac–At (<2 μm) corresponds to a kaolinite.

3.4. *^{29}Si and ^{27}Al-magic angle spinning neutron magnetic resonance (^{29}Si MAS NMR and ^{27}Al MAS NMR)*

3.4.1. *^{29}Si MAS NMR*

The spectra for both fractions of Te–Tl (<1 μm and 2–1 μm, Fig. 7), showed broad peaks due to the heteronuclear bipolar interactions of ^{29}Si with ^{1}H and ^{27}Al that define amorphous sites characteristic of aluminosilicates. This amorphous environment for the silicon atoms is observed in soils with halloysite, and can be explained by the presence of hydration water and OH hydroxyl groups (Engelhardt and Michel, 1987). In the ^{29}Si NMR spectra, a signal centered at −104 ppm was observed. This signal indicates mainly the existence of Q^4 species (4 Si atoms linked to a SiO_4 tetrahedral), and the enveloping one includes also Q^3 species that are not clearly defined. This peak is similar in intensity and width in the two fractions studied.

Another peak due to Q^2 (groups $(Si(OSi)_2(OH)_2)$ is observed in the spectra of soils analyzed at −85 ppm. The Q^2/Q^4 ratio is slightly higher in the Te–Tl (<1 μm) spectrum (Fig. 7A) than in the 2–1 μm sample (Fig. 7B). The greater proportion of Q^2 units in Te–Tl (<1 μm) than in Te–Tl (2–1 μm) is associated with the increase of alumino-silicated structures in that finer fraction, completely made up of clay minerals of the type 1:1, presumably halloysites, according to FTIR. The fraction (2–1 μm) with a lower proportion of Q^2 species corresponded to a mixture of albite + crystoballite + halloysite, according to XRD. This spectrum was very similar to that presented by Kodama et al (1989) for clay minerals (<2 μm).

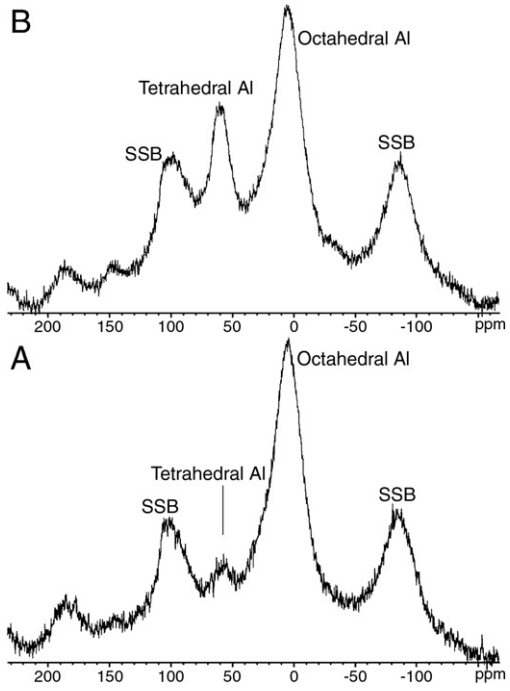

Fig. 8. ^{27}Al magic angle spinning nuclear magnetic resonance spectra from Te–Tl, (A) <1 μm and (B) 2–1 μm.

3.4.2. *^{27}Al MAS NMR*

The spectra for both fractions of Te–Tl (<1 μm and 2–1 μm, Fig. 8) showed broad peaks due to the tetrahedral and octahedral aluminum species in an amorphous context.

The octahedral species predominate in both spectra. The chemical shifts corresponding to octahedral and tetrahedral orderings of Te–Tl (2–1 μm) (Fig. 8B) showed a displacement in its position towards low fields. This indicates that one of more silicon atoms are being replaced by aluminum in the external coordination sphere of Q^4. As previously indicated, this observation is associated with the abundance of SiO_4 units surrounded by Al atoms (Engelhardt and Michel, 1987). In

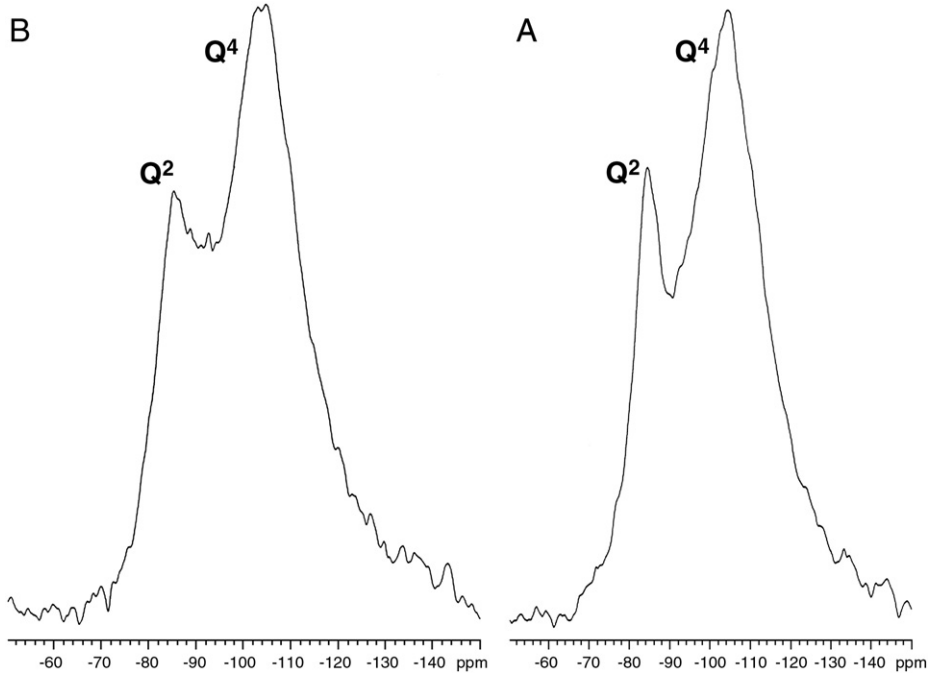

Fig. 7. ^{29}Si magic angle spinning nuclear magnetic resonance spectra from Te–Tl, (A) <1 μm and (B) 2–1 μm.

addition, the peak corresponding to Al^{IV} tetrahedral ordering was bigger in Te–Tl (2–1 μm) (Fig. 8B) than in Te–Tl (<1 μm) (Fig. 8A), which indicates more abundance of Al^{IV} in the thicker fraction (2–1 μm) (Engelhardt and Michel, 1987). This is attributed to the presence of albite in this thicker fraction, this alkali feldspar shows Al^{IV} in its crystalline network (Merino et al., 1989) and spectra with a peak at approximately 55 ppm for ^{27}Al (Kirkpatrick, 1988), contributing to a higher amount of tetrahedral aluminum. In the case of albite, the observed ^{27}Al chemical shift is associated with the substitution of A1 for Si in one out of four tetrahedrons (Kirkpatrick, 1988).

The abundance of Al^{IV} in spectra of ^{27}Al MNR MAS has been also reported by Kodama et al. (1989). This effect was explained as a result of the deshidroxylation (loss of OH groups) of a kaolinite sample, going from an original coordination of $Al^{VI}(OH)_4O_2$ to $Al^{IV}O_4\square_z$ where □ indicates a vacancy due to the absence of a ligand.

The results from ^{29}Si MAS NMR and ^{27}Al MAS NMR showed that <1 μm fraction from Te–Tl is completely made up of clay minerals of the type 1:1 type halloysite. In the case of the thicker fraction 2–1 μm, it confirms the mixture of albite + cristobalite + halloysite, according to XRD.

3.5. Electron microscopy (TEM and HRTEM)

The form of the clays of the Te–Tl<1 μm fraction was similar to those reported in the literature for tubular halloysite (Fig. 9) (Dixon and McKee, 1974; Nagasawa and Miyazaki, 1975; Ross et al., 1983; Singh and Gilkes, 1992; Romero et al., 1992).

A representative HRTEM image (Fig. 10) of this clay fraction exhibits basal lattice fringes.

The layers present apparently uniform contrast and orientation, however closer examination in a selected area reveals small differences in the layer spacing. This is presented in Fig. 11.

Such an intensity profile shows the position of the layers with respect to distance. Packets of seven or six layers can be found in similar distances in the image, suggesting that a different phase fills up the space between layers. Filtering of the original image can be used to better appreciate the periodicity of layer spacing. Fig. 12 shows a filtered image; the filtering has been done on the Fourier transform by selecting exclusively the periodic maxima as shown in the insert of the last figure.

In addition to the presence of packets with different numbers of layers in a given distance, a slight deformation of the layers can be noticed. This strain can also be explained by a different phase located between the layers. Other areas in the investigated sample show defects; an example is given in Fig. 13 indicated by a square area.

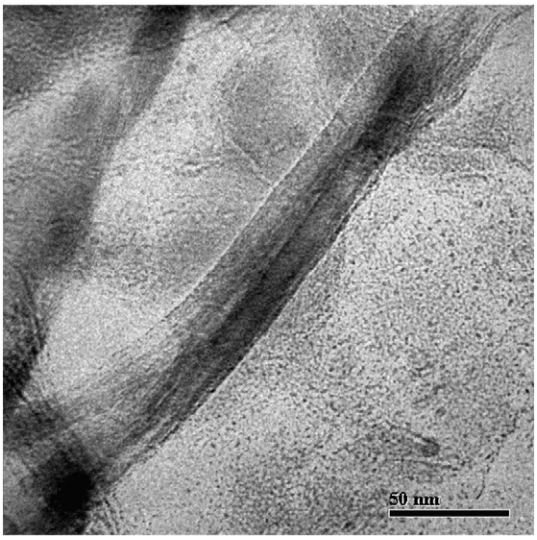

Fig. 9. TEM image from Te–Tl, <1 μm, showing the form of the clay.

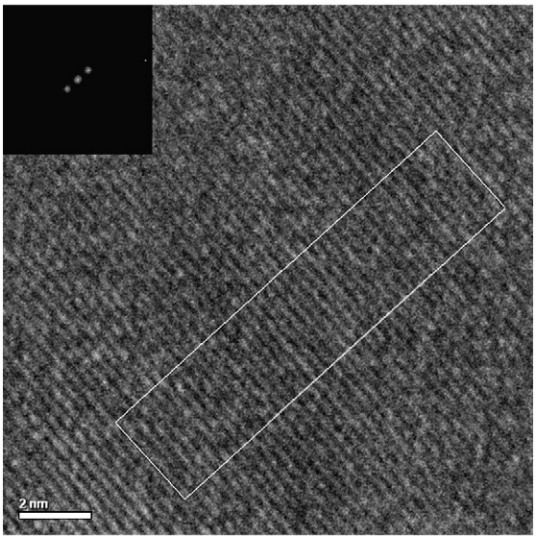

Fig. 10. Representative HRTEM image from Te–Tl, <1 μm, showing a selected area with apparently uniform basal lattice fringes. Fourier transform from the image.

There is a lateral layer termination and the corresponding deformation. This has been also observed by Ma and Eggleton (1999). According to Chukhrov and Zvyagin (1966), the tubular halloysite is really made up of kaolinite sheets, which displace in a disorderly fashion one upon the other, generating structural disorder. Ma and Eggleton (1999) have reported structural defects similar to those observed in kaolinite particles. In all cases, the Fourier transform was obtained from the image.

In order to determine the composition of the particles studied, the development of a microanalysis study was attempted; yet the apparently very fine sheets rapidly disintegrated under the electron beam. This characteristic of the type 1:1 clay has been reported in literature, which makes it difficult to study it at that level.

3.6. Chemical analyses

Chemical analyses were only made on the Acrisol sample (Ac–At). The percentage of Fe extracted with OXA (Fe_{OXA}) was 0.773%, indicating a low content of poorly ordered iron oxides such as ferrihydrite (Mizota and van Reeuwijk, 1989). An estimation of ferrihydrite (1.31%) was obtained using the estimate suggested by Childs (1985) (% ferrihydrite = % Fe_{OXA} * 1.7). On the contrary, the Fe extracted with DCB (Fe_{DCB}) was higher (5.57%), showing that the Ac–At sample is made up mainly of crystalline iron oxides and oxyhydroxides (goethite and hematite), in addition to Fe in organic complexes. The extraction of Fe with PYR

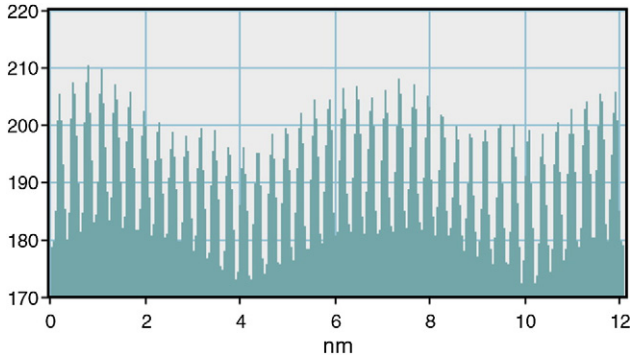

Fig. 11. Distribution of profile layers spacing showing the packets of layers in similar distances.

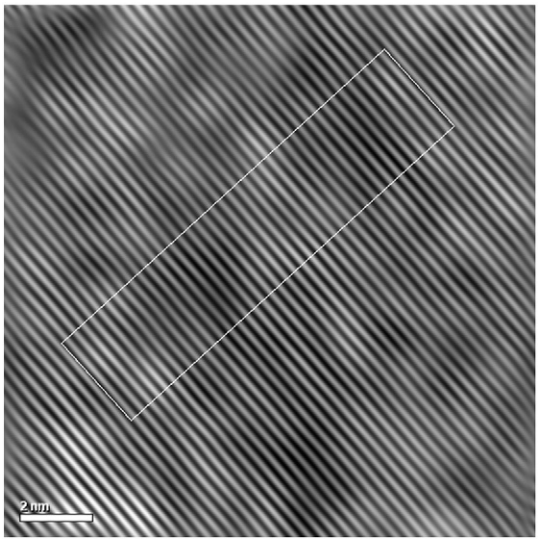

Fig. 12. Filtered image on the Fourier transform showing in detail the periodicity of layer spacing in a selected area.

(Fe_{PYR}) showed that only a small percentage of Fe (0.15%) corresponds to Fe in organic complexes (Mizota and van Reeuwijk, 1989). The Fe_{OXA}/Fe_{DCB} relation or "activity ratio" has been widely used as an index for the degree of crystallinity or "age of iron oxides". In Ac–At, this relation was 0.14, very close to 0.1, a value reported by Andriesse (1978) for Oxisols and which a number of authors have suggested for old soils.

3.7. Mössbauer spectroscopy (MS)

The Mössbauer spectrum of the Ac–At fraction (<2 μm) was presented in Fig. 14. In this one, two unfoldings associated with the akaganeite (β-FeOOH) (corresponding to Fe^{3+}) were observed, as well as another two small quadrupoles associated with the hematite (α-Fe_2O_3) and the goethite (α-FeOOH), which indicated the existence of these iron minerals.

Fitted parameters at 295 K obtained for the four characterized Fe-mineral species are shown in Table 1. The relative area (A) indicated that the akaganeite was the most abundant species (87.58%) in the fraction studied, and the hematite and goethite were present in a lower proportion, 11.06% and 1.37%, respectively. The high values of

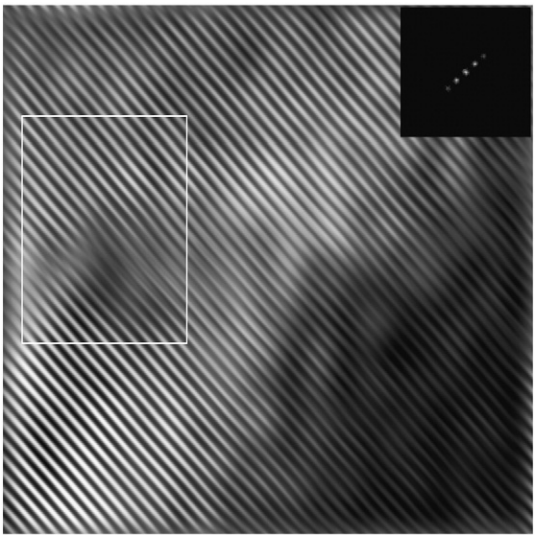

Fig. 13. Representative HRTEM image showing deformation defects of lattice fringes in the square area. Fourier transform from the image.

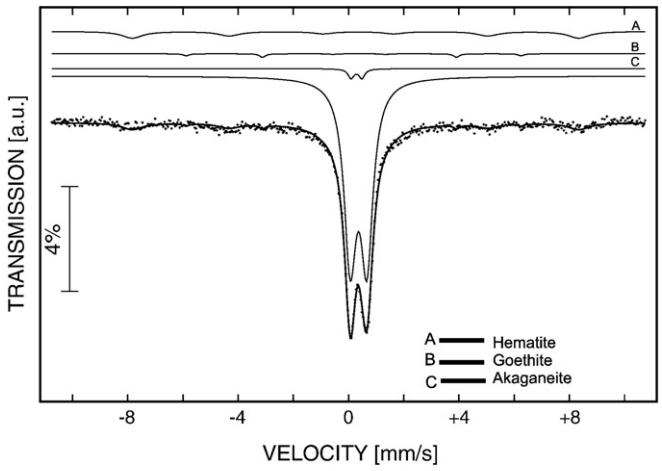

Fig. 14. Mössbauer spectrum from Ac–At, <2 μm.

the hyperfine magnetic field, (H_f) of 37.8 T and 51.3 T, corroborated the presence of goethite and hematite in the fraction under study. These values have been reported by other authors. The quadrupole splitting (Δ) for the goethite and the hematite was negative (−0.21 and −0.107 mm s^{-1}, respectively) and positive for the akaganeite (0.32 and 0.39 mm s^{-1}).

4. Discussion

4.1. Tepetate Te–Tl

The studies with ^{29}Si and ^{27}Al MAS NMR confirmed that the phyllosilicate minerals reported in the Te–Tl (<1 μm and 2–1 μm fractions) do not correspond to a kaolinite. The spectra found in literature for the latter only indicate the Q^4 sign, approximately −90 ppm, for ^{29}Si (Engelhardt and Michel, 1987; Kodama et al., 1989) and for ^{27}Al a sign between −91.5 and −98.5 ppm corresponding to Al^{VI} (Engelhardt and Michel, 1987; Kodama et al., 1989). The ^{27}Al spectrum does not correspond to metakaolin either, even though two of the three peaks characteristic of this mineral (Al^{IV}, 50 ppm and Al^{VI}, −4.1 ppm) appear, the one corresponding to 30 ppm (Al^{IV}) does not (Kodama et al., 1989). Nevertheless, there is certain discrepancy in this last sign, which Mackenzie et al. (1985) associated with a separate tetrahedral species (Kodama et al., 1989). The spectra do not correspond either to those reported by Wada et al. (1988) and Satokawa et al. (1994) for spherical halloysites, with a sign for ^{29}Si at −93 ppm and two peaks at 56–66 ppm and 0–3 ppm for ^{27}Al. According to Singh and Gilkes (1992), the halloysites derived from crystalline minerals like feldspar and micas exhibit a tubular morphology. On the other hand, these halloysites, generally derived from volcanic glass, show a spheroidal morphology (Singh and Gilkes, 1992).

The main structural feature shown by the ^{27}Al MAS NMR was the substitution in the halloysite of Al^{IV} for Si, which is a tendency coming from the 1:1 layers of the mineral (Merino et al., 1989). According to some scientists, there is a relationship between the halloysite tubular morphology and the substitution of Al^{IV} for Si (Komarneni et al., 1985). Chemical studies like those developed by Newman and Brown

Table 1
Mössbauer parameters from Ac–At, <2 μm fraction.

Minerals	δ(Fe) [mm s^{-1}]	Δ [mm s^{-1}]	H_f [T]	Relative area [%]
Hematite (α-Fe_2O_3)	0.31	−0.107	51.3	11.06
Goethite (α-FeOOH)	0.29	−0.21	37.8	1.37
Akaganeite (β-FeOOH)	−0.12	0.32	–	85.43
	−0.10	0.39	–	2.15

Isomer shift (δ) values relative to α-Fe at 298 K, (δ): isomer shift, (Δ): quadrupole splitting, (H_f) : hyperfine magnetic Field, (A): relative area.

(1987) and others indicated that most of the halloysites analyzed present Al/Si relations higher than the unit, which reveals the presence of Al^{IV} in the tetrahedron layer (Merino et al., 1989).

According to Merino et al. (1989), there is a genetic link between: (1) the chemical composition of the halloysite (with significant Al^{IV} and connected monovalent cations), (2) the tubular morphology and (3) the composition of the solution (pH, $mAl_{(total)}$, m_{M+}, m_{SiO_2}). These authors consider that similar links can be present in other minerals. Our observations in FTIR and ^{27}Al MAS NMR confirmed the relationship between the halloysite tubular morphology and the substitution of Al^{IV} for Si (Komarneni et al., 1985; Merino et al., 1989). Yet other authors think it is difficult to explain the morphology of halloysites on the basis of one single factor because of the great diversity of agents and conditions taking part in the genesis of these clays (Romero et al., 1992).

The HRTEM observations showed halloysites with an apparently tubular form, which would confirm in an independent manner that these derived from feldspar (Singh and Gilkes, 1992), but studies of the tubes using cross section are recommended. Studies with HRTEM and MET (Singh and Gilkes, 1992; Bobos et al., 2001; Huertas et al., 2004) have revealed that tubular and spherical particles, commonly defined as halloysites, may result from the rolling of kaolinite sheets, which may lead to a number of mistakes. According to Bailey (1989), many particles with this morphology, characterized as halloysites, are likely to have actually been kaolinites. The formation conditions of both clays are very similar, which has meant slight differences set out in literature, not always easy to define between the two (Huertas et al., 2004). On this account, the characterization of the fraction <1 μm of Te–Tl from the HRTEM proved to be inconclusive.

The most important result obtained from the HRTEM observations was the evident structural disorder of the halloysite, shown by the lateral layer termination and deformations (Ma and Eggleton, 1999). The halloysite has been considered the last member of the kaolinite series, with a more disordered structure (Chukhrov and Zvyagin, 1966). The structural disorder observed would then be a product of hydration of the kaolinite sheets (Wada, 1961; Chukhrov and Zvyagin, 1966; Constanzo et al., 1984), but also of the substitutions of Al^{IV} in the tetrahedrons (Kodama et al., 1989). The studies developed by Drever (1982) showed that the substitution of Al^{IV} for Si in the halloysite causes a bending of the sheet layers.

The presence of albite (Na,Ca) $(Si,Al)_4O_8$ in the 2–1 μm fraction of the Te–Tl *tepetate* leads to the assumption that the observed halloysite was formed from the alteration of these minerals. The formation of halloysites from feldspar weathering has been documented in literature (Bates, 1962; Parham, 1969; Eswaran and Bin, 1978; Kirkman, 1981; Anand et al., 1985; Banfield and Eggleton, 1990; Singh and Gilks, 1992; Wilson, 2004).

With the results obtained it is difficult to trace a probable route of the genesis of the halloysite identified in the fine fractions of Te–Tl. However, it has been pointed out that the transition from kaolinite to halloysite-7 Å is expressed by the reduction of the structural order and the increase of the structural water content (Bobos et al., 2001), characteristics found in the structure of the Te–Tl halloysite. The formation of the tubular halloysite is explained by the loss of rigidity in some points along the kaolinite crystal (Robertson and Eggleton, 1991), deforming the sheets of the latter (Singh and Gilkes, 1992).

The transformation from halloysite-7 Å into kaolinite (Churchman and Gilkes, 1989) in lateritic profiles of dolerite and granite (Bobos et al., 2001) has also been reported. Other documented mechanisms for the formation of tubular halloysite are: (1) the result of the crystallization of the solution (Bates et al., 1950; Kirkman, 1981), an explanation that was questioned by Bailey (1989), who reported the development of tubes through processes of deformation of flat pseudomorph of kaolinite after mica, rather than as a result of the growth of crystals of the solution (Singh and Gilkes, 1992); (2) elongated tubes of halloysite-7 Å have been genetically related to gels of Si–Al resulting from the dissolution of feldspars, as well as the presence of short tubes has been associated with the rolling (folding/rolling) of kaolinite plates (Bobos et al., 2001).

4.2. Acrisol–Atécuaro (Ac–At)

The presence of iron oxides has shown to influence soil aggregation (Goldberg, 1989), however goethite and hematite (Fe_{DCB}) are less effective aggregating material than ferrihydrite (Fe_{OXA}) (Arduino et al., 1989). The presence in Ac–At of a larger proportion of Fe_{DCB} than Fe_{OXA} leads to the assumption that these soils are susceptible to erosion (Rhoton et al., 1998). The akaganeite (β-FeOOH), a mineral with the same composition of the goethite and the lepidocrocite, but structurally different, was reported to be present in the soil (Schwertmann and Taylor, 1989). The studies with XRD and FTIR confirmed that the phyllosilicate minerals reported in the Ac–At (<2 μm fraction) correspond to a kaolinite.

5. Conclusions

The above results show that the fine (<1 μm) and the coarse (2–1 μm) fractions of Te–Tl consist largely of partially dehydrated 0.7-nm halloysite supposedly tubular; the latter presents also cristobalite, quartz and albite. Ac–At is made up of kaolinite, goethite, hematite, akaganeite (β-FeOOH), cristobalite and quartz.

Even when there is a lack of consistency in the terminology and criteria used to distinguish between kaolinite and halloysite, as pointed out by Churchman and Gilkes (1989), this study is aimed to contribute to the presentation of ^{27}Al and ^{29}Si MAS NMR and FTIR spectroscopy as a set of successful procedures in the characterization of halloysites in the soil. The traditional procedure to distinguish the differences between kaolinites and halloysites, which is the XRD after the treatment with formamide (Churchman et al., 1984), is not sufficiently precise if other phillosilicates (10 Å and 14 Å) are present (Romero et al., 1992). The MET and HRTEM electron microscopy techniques, which are proposed as alternatives, are still not very accessible due to the few experts on this subject engaged in the study of the soil; in addition to the fact that these are costly techniques.

Apparently this is the first time that iron oxides composition in Mexican soils using Mössbauer spectroscopy (MS) is reported. The results obtained by MS in Ac–At showed that akaganeite is the principal Fe-mineral component and there are also less quantity of goethite and hematite. Ferrihydrite (poorly crystalline Fe oxide) is also present in low percentage. However, the presence of akaganeite must be confirmed by other more thorough studies as it is a mineral whose presence in soils is not commonly reported. The location of the sampling site in an ancient volcanic crater might justify its presence as it has been detected in mineral deposits (Schwertmann and Taylor, 1989).

The fine fractions of the degraded soils included in this study are made up of low activity clays: tubular halloysites in the Te–Tl *tepetates* and kaolinites in Ac–At. For this reason, the restoration techniques proposed for these degraded soils must be complemented with fertilization practices providing basic elements (Ca, Mg, K and Na) to the soil, which shows a deficit due to the low activity of the fine fraction.

Clays have been reported to show different mechanisms of association with soil organic matter, in accordance with their nature, and clay mineralogy is a determinant factor in the turnover times of C in the soil (Wattel-Koekkoek et al., 2001, 2003). Acrisols (soils with kaolinite) included in this study show a potential source of soil carbon sequestration because organic matter is free or associated with hydroxide surfaces, there is little information about halloysites in relation to their potential for carbon sequestration. In further studies to focus on the relationship between mineralogy and the latter phenomenon it will be necessary to clarify the characteristics of the fine fraction of the soil (<2 μm), considered to be the most active in the sequestration process.

Acknowledgements

Thanks are due to the CONACYT Project 408899-Z and REVOLSO project ICA4-CT-2001-10052 for the financial support given for the development of experiments. To Jean Marc Lapetite del Laboratoire d´Étude des Transferts en Hydrologie et Environnement (LTHE) from the IRD, Grenoble, France, to Leticia Baños from UNAM-Mexico for the XRD support and Karla A. Barrera Rivera from the University of Guanajuato for their collaboration in the obtention of some of the results of this work.

References

Anand, R.R., Gilks, R.J., Armitage, T., Hillyer, J., 1985. The influence of microenvironment on feldspar weathering in lateritic saprolite. Clays and Clay Minerals 33, 31–46.
Andriesse, J.P., 1978. A study into the mobility of iron in podzolized Serawak upland soils by means of selective iron extraction. Netherland Journal Agricultural Science 27, 1–12.
Arduino, E., Barberis, E., Boero, V., 1989. Iron oxides and particle aggregation in B horizons of some Italian soils. Geoderma 45, 319–329.
Bailey, S., 1989. Halloysite. A critical assessment. Proceedings of the 9th International Clay Conference: Strasbourg, Sciences Géologiques, Mémoire, vol. 86, pp. 89–98.
Banfield, J.F., Eggleton, R.A., 1990. Analytical transmission electron microscope studies of plagioclase, muscovite and K-feldspar weathering. Clays and Clay Minerals 38, 77–89.
Barnhisel, R.I., Bertsch, P.M., 1989. Chlorites and hydroxy-interlayered vermiculite and smectite, In: Dixon, G.G., Weed, Y.Y. (Eds.), Minerals in Soil Environments, 2nd Edition. Soil Science Society of America, Madison WI, USA, pp. 729–745.
Bates, T.F., 1962. Haloysite and gibbsite formations in Hawaii. Clays Clay Minerals 9, 315–328.
Bates, T.F., Hildebrand, F.A., Swineford, A., 1950. Morphology and structure of endellite and halloysite. American Mineralogist 6, 237–248.
Bobos, I., Duplay, J., Rocha, J., Gomes, C., 2001. Kaolinite to halloysite-7 Å transformation in the kaolin deposit of São Vicente de Pereira, Portugal. Clays and Clay Minerals 49, 596–607.
Brady, N., Weil, R.R., 2002. The Nature and Properties of Soils, Thirteen ed. Prentice Hall, New Jersey, USA. Chapter 19.
Brindley, G.W., 1980. In: Brindley, G.W., Brown, G. (Eds.), Order–disorder in the clay mineral structures. : Crystal Structures of Clay Minerals and their X-ray Identification Monograph, vol. 5. Mineralogical Society, London, pp. 125–196.
Brindley, G.W., Robinson, K., 1946. Randomness in the structures of kaolinite clay minerals. Transactions of the Faraday Society 42B, 198–205.
Brown, G., Brindley, G.W., 1980. X-ray diffraction procedures for clay minerals identification. In: Brindley, G.W., Brown, G. (Eds.), Crystal Structures of Clay Minerals and Their X-ray Identification. Mineral Society, London, pp. 305–359.
Chen, P.Y., 1984. Distribution and origin of clay minerals in the shallow sea surrounding the Chinmen Island (Quemoy), Fukien, China. Proceedings of the Geological Society of China 27, 101–118.
Chen, P.Y., Lin, M.-L., Zheng, Z., 1997. On the origin of the name kaolin and the kaolin deposits of the Kauling and Dazhou areas, Kiangsi, China. Applied Clay Science 12, 1–25.
Chen, P.Y., Wang, M.K., Yang, D.S., Chang, S.S., 2004. Kaolin minerals from Chinmen Island (Quemoy). Clays and Clay Minerals 52, 130–137.
Childs, C.W., 1985. Towards understanding soil mineralogy. II. Notes of ferrihydrite. Laboratory Report CM7. Soil Bureau, Lower Hutt, New Zealand.
Chukhrov, F.V., Zvyagin, B.B., 1966. Halloysite a cristallochemically and mineralogically distinct species. In: Heller, L., Weiss, A. (Eds.), Procedings of the Internacional Clay Conference Jerusalem: Israel Prog. Sci. Transl., Jerusalem, vol. 1, pp. 11–25.
Churchman, G.J., Gilkes, R.J., 1989. Recognition of intermediates in the possible transformation of halloysites to kaolinites in weathering profiles. Clay Minerals 24, 579–590.
Churchman, G.J., Whitton, J.S., Claridge, G.G.C., Theng, B.K.G., 1984. Intercalation method using formamide for differentiating halloysite from kaolinite. Clays and Clay Minerals 32, 241–248.
Constanzo, P.M., Giese, R.F., Lipsicas, M., 1984. Static and dynamic structure of water in hydrated kaolinites. I. The static structure. Clays and Clay Minerals 32, 419–428.
Covaleda, S., Pajares, S., Gallardo, J., Etchevers, B.J.D., 2006. Changes in C and N distribution in soil particle size fractions induced by agricultural practices in a cultivated volcanic soil from Mexico. Organic Geochemistry 37, 1943–1948.
Dixon, J.B., McKee, T.R., 1974. Internal and external morphology of tubular and spheroidal halloysite particles. Clays and Clay Minerals 22, 127–137.
Drever, J.I., 1982. The Geochemistry of Natural Waters. Prentice-Hall, Englewood Cliffs, N.J.
Engelhardt, G., Michel, D., 1987. High-Resolution Solid State NMR of Silicates and Zeolites. John Wiley and Sons, Great Britain.
Eswaran, H., Bin, W.C., 1978. A study of deep weathering profile on granite in peninsular Malaysia: II. Mineralogy of the clay, silt and sand fractions. Soil Science of America Journal 42, 149–158.
Etchevers, J.D., Hidalgo, C., Prat, C., Quantin, P., 2006. Tepetates of Mexico, In: Lal, R. (Ed.), Encyclopedia of Soil Science, Second edition. Marcel Dekker, New York.
FAO, 1979. A Provisional Methodology for Soil Degradation Assessment. FAO, Roma.
FAO, 1994. Land degradation in South Asia: its severity, causes and effects upon the people. : World Soil Resources Report, vol. 78. FAO, Roma.
Farmer, V.C., 1974. The layer silicates. In: Farmer, V.C. (Ed.), The Infrared Spectra of Minerals. Mineralogical Society, London, UK, pp. 331–363.
Farmer, V.C., 1979. Infrared spectroscopy. In: van Olphen, H., Fripiat, J.J. (Eds.), Data Handbook for Clay Minerals and Other Non-metallic Minerals. Pergamon Press, New York.
Fröhlich, F., 1993. La silice sédimentaire: structure des verres d´origine biologique et quantification de la sílice dans les roches. Spectroscopie infrarouge et analyse minéralofique quantitative des roches. : Journée d´étude. ORSTOM, Bondy, France, pp. 59–64.
Frost, R.L., 1998. Hydroxyl deformation in kaolins. Clays and Clay Minerals 46, 280–289.
Goldberg, S., 1989. Interaction of aluminum and iron oxides and clay minerals and their effect on soil physical properties: a review. Communications in Soil Science and Plant Analysis 20, 1181–1207.
Hessmann, R., 1992. Micromorphological investigations on “tepetate” formation in the “toba”-sediments of the state of Tlaxcala (Mexico). Terra 10 (Número especial), 145–150.
Hidalgo, C., 1996. Ètude d´horizons indurés à comportement de fragipan, appelés tepetates, dans les sols volcaniques de la vallée de Mexico. Contribution à la connaissance de leurs caractères et de leur formation. Thèses et documents microfiches, No. 146, Orstom-Èditions, Paris. 215 p.
Van der Marel, H.W., Beutelspacher, H., 1976. Atlas of Infrared Spectroscopy of Clay Minerals and Their Admixtures. Elsevier, Ámsterdam.
Hidalgo, C., Quantin, P., Zebroski, C., 1992. La cementación de los tepetates: estudio de la silicificación. Terra 10 (Número especial), 192–201.
Hidalgo, C., Elsass, F., Quantin, P., Thiry, M., 1997. Nanoorganisation des argiles et des formes de silice dans des tepetates de type fragipan (Vallée de Mexico). In: Elsass, F., Jaunet, A.M. (Eds.), Structure et ultrastructure des sols et des organisms vivants. Paris, pp. 121–135. INRA Editions.
Holtzapffel, T. 1985. Les minéraux argileux. Société géologique du Nord. Publication n°. 12. S.G.N. Villeneuve D´Ascq, France.
Huertas, F.J., Fiore, S., Linares, J., 2004. In situ transformation of amorphous gels into spherical aggregates of kaolinite: a HRTEM study. Clay Minerals 39, 423–431.
Joussein, E., Petit, S., Churchman, J., Theng, B., Righi, D., Delvaux, B., 2005. Halloysite clay minerals — a review. Clay Minerals 40, 383–426.
Kirkman, J.H., 1981. Morphology and structure of halloysite in New Zealand tephras. Clays and Clay Minerals 29, 1–9.
Kirkpatrick, R.M., 1988. MAS NMR spectroscopy of minerals and glasses. In: Hawthorne, F.C. (Ed.), Spectroscopic Methods in Mineralogy and Geology: Mineralogical Society of America, Reviews in Mineralogy, vol. 18, pp. 341–387.
Kodama, H., Oinuma, J., 1963. Identification of kaolin minerals in the presence of chlorite by X-ray diffraction and infrared absorption spectra. Clays Clay Minerals 11, 236–249.
Kodama, H., Kotlyar, L.S., Ripmeester, J.A., 1989. Quantification of crystalline and noncrystalline material in ground kaolinite by X-ray powder diffraction, infrared, solid-state nuclear magnetic resonance, and chemical-dissolution analyses. Clays and Clay Minerals 37, 364–370.
Komarneni, S., Fyfe, C., Kennedy, G.J., 1985. Order–disorder in 1:1 type clay minerals by solid-state ^{27}Al and ^{29}Si magic-angle spinning NMR spectroscopy. Clay Minerals 20, 327–334.
Ma, Ch., Eggleton, R.A., 1999. Surface layer types of kaolinite a high-resolution transmission electron microscope study. Clays and Clay Minerals 47, 181–191.
Mackenzie, K.J.D., Brown, I.W.N., Meinhold, R.H., Bowden, M.E., 1985. Outstanding problems in the kaolin-mullite reaction sequence investigated by ^{29}Si and ^{27}Al solid-state nuclear magnetic resonance: I. Metakaolinite. Journal American Ceramic Society 68, 293–297.
Madejová, J., Komadel, P., 2005. Information available from infrared spectra of the fine fractions of bentonites. In: Kloprogge, T. (Ed.), The Application of Vibrational Spectroscopy to Clay Minerals and Layered Double Hydroxides. : CMS Workshop Lectures, vol. 13. The Clay Minerals Society, Aurora, CO, pp. 66–98.
Mehra, O.P., Jackson, M.L., 1960. Iron oxide removal from soils and clays by a dithionite–citrate system buffered with sodium bicarbonate. Clays Clay Minerals 5, 317–327.
Merino, E., Harvey, C., Murray, H.H., 1989. Aqueous-chemical control of the tetrahedral-aluminum content of quartz, halloysite, and other low-temperature silicates. Clays and Clay Minerals 37, 135–142.
Miehlich, G., 1992. Formation and properties of tepetate in the central highlands of Mexico. Terra 10 (Número especial), 137–144.
Mizota, C., van Reeuwijk, L.P., 1989. Clay mineralogy and chemistry of soils formed in volcanic material in diverse climatic regions. : Soil Monograph, vol. 2. International Soil Reference and Information Center (ISRIC), Wageningen, The Netherlands.
Moore, D.M., Reynolds Jr., R.C., 1997. X-ray Diffraction and the Identification and Analysis of Clay Minerals. Oxford University Press, Oxford, New York.
Nagasawa, K., Miyazaki, S., 1975. Mineralogical properties of halloysite as related to its genesis. Proceedings of the International Clay Conference. Applied Publishing Ltd, Wilmette, Illinois, U.S.A.
Newman, A.C.D., Brown, G., 1987. The chemical constitution of clays. In: Newman, A.C. D. (Ed.), Chemistry of Clays and Clay Minerals. Mineralogical Society, London, pp. 1–128.
Oleschko, K., Zebrowski, C., Quantin, P., Fedoroff, N., 1992. Patrones micromorfológicos de organización de arcillas en tepetates (México). Terra 10 (Número especial), 183–191.
Parham, W.E., 1969. Formation of halloysite from feldspar: low temperature, artificial weathering versus natural weathering. Clays Clay Minerals 17, 13–22.
Poetsch, T., Arikas, K., 1997. The micromorphological appearance of free silica in some soils of volcanic origin in central Mexico. In: Zebrowski, C., Quantin, P., Trujillo, G. (Eds.), Suelos volcánicos endurecidos. ORSTOM, Ecuador, pp. 56–64.
Quantin, P., 1992. L'induration des materiaux volcaniques pyroclastiques en Amerique Latine: processus gologiques et pedologiques. Terra 10 (Número especial), 24–33.

Quantin, P., 1993. Spectroscopie IR de formes d´allophane, imogolite et halloysite des sols derives de materiaux volcaniques. Spectroscopie infrarouge et analyse minéralogique quantitative des roches. : Journée d´étude. ORSTOM, Bondy, France, pp. 39–51.

Quantin, P., Herbillon, A.J., Janot, C., Siefferman, G., 1984. L''halloysite' blanche riche en fer de Vate (Vanuatu). Hypothèse d'un edifice interstratifie halloysite–hisingerite. Clay Minerals 19, 629–643.

Quantin, P., Zebrowski, C., Delaune, M., Hidalgo, C., 1992. El material original de los tepetates t2 y t3 de la región de Texcoco (México): ¿loess o cineritas?. Terra 10 (Número especial), 178–182.

Rhoton, F.E., Lindbo, D.L., Römkens, M.J.M., 1998. Iron oxides erodibility interactions for soils of the Memphis Catena. Soil Science Society of America 62, 1693–1703.

Robertson, I.D., Eggleton, R.A., 1991. Weathering of granitic muscovite to kaolinite and halloysite and plagioclase derived kaolinite to halloysite. Clays and Clay Minerals 39, 113–126.

Romero, R., Robert, M., Elsass, F., Garcia, C., 1992. Abundance of halloysite neoformation in soils developed from crystalline rocks. Contribution of transmission electron microscopy. Clay Minerals 27, 35–46.

Ross, G.J., Kodama, H., Wang, C., Gray, J.T., Lafreniere, L.B., 1983. Halloysite from a strongly weathered soil at Mont Jacques Cartier, Quebec. Soil Science Society of America Journal 47, 327–332.

Satokawa, S., Osaki, Y., Samejima, S., Miyawaki, R., Tomura, S., Shibasaki, Y., Sugahara, Y., 1994. Effects of the structure of silica–alumina gel on the hydrotermal synthesis of kaolinite. Clays and Clay Minerals 42, 288–297.

Sawhney, B.L., 1989. Interstratification in layer silicates. In: Dixon, J.B., Weed, S.B. (Eds.), Minerals in Soil Environments. Soil Science Society of America, Madison, WI, pp. 789–827.

Schwertmann, U., Taylor, R.M., 1989. Iron Oxides, In: Dixon, J.B., Weed, S.B. (Eds.), Minerals in Soil Environment, 2nd edition. Soil Science Society of America, Madison, Wisconsin, pp. 379–438.

SEMARNAT-CP. 2001. Memoria Nacional. Evaluación de la degradación de los suelos causada por el hombre en la República Mexicana, a escala 1:250,000. Secretaría de Medio Ambiente y Recursos Naturales y Colegio de Postgraduados. México, D. F.

Singh, B., Gilkes, R.J., 1992. An electron optical investigation of the alteration of kaolinite to halloysite. Clays and Clay Minerals 40, 212–229.

Theng, B.K.G., Russell, M., Churchman, G.J., Parffit, R.L., 1982. Surface properties of allophane, halloysite and imogolite. Clays and Clay Minerals 30, 143–149.

Trunz, V., 1979. The influence of crystallite size on the apparent basal spacings of kaolinite. Clays and Clay Minerals 24, 84–87.

Van Reeuwijk, L.P., 1995. Procedures for soil analysis. Technical paper No. 9. International Soil Reference and Information Centre, Wageningen, Netherlands.

Wada, K., 1961. Lattice expansion of kaolin minerals by treatment with potassium acetate. American Mineralogist 46, 78–91.

Wada, K., Wilson, M., Kakuto, Y., Wada, S.-I., 1988. Synthesis and characterization of a hollow spherical form of monolayer aluminosilicate. Clays and Clay Minerals 36, 11–18.

Wattel-Koekkoek, E.J.W., van Genuchten, P.P.L., Buurman, P., van Lagen, B., 2001. Amount and composition of clay-associated soil organic matter in a range of kaolinite and smectite soils. Geoderma 99, 27–49.

Wattel-Koekkoek, E.J.W., Buurman, P., van der Plicht, J., Wattel, E., van Breemen, N., 2003. Mean residence time of soil organic matter associated with kaolinite and smectite. European Journal of Soil Science 54, 269–278.

Wilson, M.J., 1987. A Handbook of Determinative Methods in Clay Mineralogy. Chapman and Hall, New York.

Wilson, I.R., 2004. Kaolin and halloysite deposits of China. Clay Minerals 39, 1–15.

WRB, 2006. World Reference Base for Soil Resources. : World Soil Resources Reports, vol. 103. Food and Agriculture Organization of the United Nations, Rome, Italy. 127 pp.

Zebrowski, C., 1992. Los suelos volcánicos endurecidos en América Latina. Terra 10 (Número especial), 16–23.